Peptides at vesicle and mineral prebiotic interfaces

Ivan Cherepashuk[1], Mikhail Makarov[1], Radko Soucek[2], Robin Krystufek[2], Romana Hadravova[2], Valerio Guido Giacobelli[1,2], Liam M. Longo[3,4], Kosuke Fujishima[3,6*], Sean F. Jordan[5*], Klara Hlouchova[1,2*]

[1] *Department of Cell Biology, Faculty of Science, Charles University, Prague 12800, Czech Republic*

[2] *Institute of Organic Chemistry and Biochemistry, Czech Academy of Sciences, Prague 16610, Czech Republic*

[3] *Earth-Life Science Institute, Institute of Science Tokyo, Tokyo 1528550, Japan*

[4] *Blue Marble Space Institute of Science, Seattle, Washington 98104, USA*

[5] *Life Sciences Institute, School of Chemical Sciences, Dublin City University, Glasnevin, Dublin, 9, Ireland*

[6] *Graduate School of Media and Governance, Keio University, Fujisawa 2520882, Japan*

*Correspondence to: fuji@elsi.jp, sean.jordan@dcu.ie, havova1@natur.cuni.cz

Abstract

The origin of life likely involved a complex interplay between organic molecules and mineral surfaces, yet the molecular details of these interactions remain poorly understood. Over recent decades, considerable research has focused on the individual roles of key biomolecules—such as RNA, lipids, and proteins—in early biogenesis. However, this reductionist view offers only a partial picture; the emergence of life likely involved networks of molecular interactions that collectively shaped early functional assemblies.

In this study, we examine the potential of peptides—arguably the most abundant early polymers—to interact with mineral surfaces and lipid vesicles, representing prebiotically plausible interfaces and compartments. Focusing on peptide compositions derived from prebiotically plausible amino acids, we demonstrate that such early peptides could bind mineral surfaces (*e.g.*, fluorapatite) via negatively charged residues. Nevertheless, the recruitment of amino acids from the modern alphabet was likely adaptive for favorable interactions with lipid vesicles and could lead to enhanced functional behavior, such as promoting phosphate release. Our findings suggest that the evolving complexity of the peptide/protein alphabet was a key factor in the evolution of protocells and could enhance early catalytic functions at the interface of geochemistry and biochemistry.

Introduction

Vesicles are believed to have been among the earliest compartmentalization structures on Earth, supporting prebiotic chemical processes essential for the emergence of life [1–6]. Similarly, minerals, known to facilitate prebiotic chemistry, may have influenced key processes such as molecular assembly, catalysis, and stabilization [7–11]. Both vesicles and mineral surfaces likely played crucial roles in shaping the chemical networks that led to life. However, while extensive research has explored vesicle and mineral physicochemical properties, much less is known about their interactions with peptides in prebiotic environments.

Multiple studies have demonstrated prebiotic feasibility of up to ~15-mer peptide synthesis under a range of conditions [12–17]. Selected di-/tri- peptides are capable of a range of catalytic activities, such as proteolytic, nucleolytic and esterase [18–20]. Specific short peptides have been moreover shown to bind decanoic acid vesicles and increase the vesicle stability to metal ions and high salt concentrations [20,21]. Although these studies imply significance of peptides in protocell evolution—whether as stabilizers, catalysts, or active participants in primitive metabolic networks - their possible role at prebiotic interfaces has not been systematically explored [21]. Before the emergence of more advanced biosynthetic pathways and full evolution of the canonical amino acid alphabet, only some amino acids were likely abundant on early Earth. Approximately half of the current canonical alphabet has been identified in plausible prebiotic environments, imitated by atmospheric discharge experiments, meteorite/asteroid analyses, and hydrothermal vent studies [22–24]. Additionally, a plethora of non-canonical amino acids was observed in prebiotic conditions and could have been incorporated in early statistical collection of peptides, before the onset of templated synthesis and selection of the life's amino acid alphabet. Compared with alternative selection from the prebiotic pool of amino acids, the "early" set of canonical residues shows exceptional distribution of volume and hydrophobicity, emulating the patterns found in the full canonical alphabet [25]. Furthermore, peptides composed of this "early" amino acid set have greater secondary structure propensity than other tested prebiotically available alternatives and would better support protein folding, despite the absence of basic residues [26,27]. These early-alphabet peptides were shown or hypothesized to be capable of metal and organic cofactor binding, interaction with RNA and potentially serve as functional hubs, bridging the gap between abiotic and enzyme catalysis [28–31].

Beyond catalysis, mineral surfaces can act as adsorption scaffolds and can prevent the "diluting out" problem of origin-of-life scenarios [7,10,32], offering a primitive form of compartmentalization Peptides frequently utilise acidic residues such as Asp and Glu for specific binding to minerals, suggesting that early canonical peptides would have the propensity to adsorb to mineral surfaces [33–37].

Fatty acid membranes and prebiotic peptides are assumed to have coexisted in the same environment (for example, fractions of Murchison meteorite were shown to self-assemble into vesicles [6]), yet what shaped their co-evolution is not yet well known. Specific peptides were shown to influence vesicle growth, morphology and stability. Hydrophobic and amphiphilic peptides integrate into lipid membranes and can promote vesicle growth and protect against disruptive effects of NaCl and divalent cations [38–43]. Individual hydrophobic amino acids like valine, isoleucine, and leucine stabilize membranes and induce lamellarity [20,38], while less hydrophobic ones, such as glycine and alanine, show weaker interactions [39,43]. Positively charged amino acids like lysine and arginine can enhance membrane stability and are crucial for membrane association and penetration

[42]. Overall, most individual amino acids exhibit some degree of interaction with fatty acid membranes [39,40,44,45].

Despite their potential significance, the interactions between peptides, vesicles, and minerals in prebiotic context remain understudied. This reflects a long-standing divide in origin-of-life research, where compartmentalization, peptide chemistry, and mineral catalysis have often been investigated separately rather than as interconnected processes [46]. Most existing studies thus far have focused on the impact of individual, shorter peptides, leaving the role of the representative prebiotic sequence space unexplored. Here we synthesize 8-mer peptide libraries representing different prebiotically plausible compositions and explore their propensity to interact with minerals and vesicles.

Results and discussion

Peptide library composition affects the extent and nature of peptide-vesicle and peptide-mineral interaction

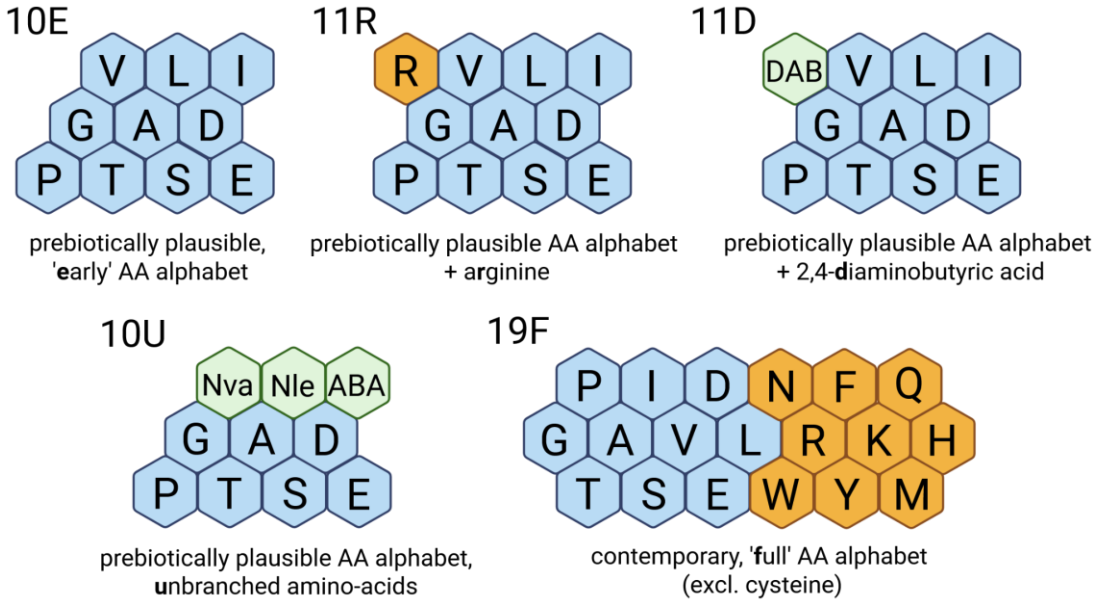

Figure 1. Composition of the analyzed random peptide libraries. All libraries were composed of 8-mers with entirely random sequences. Blue hexagons denote prebiotically available amino acids [23]; orange hexagons denote "late" amino acids that require biosynthesis; green hexagons denote prebiotically available amino acids that were not incorporated into the genetic code (non-canonical amino acids).

Representing prebiotically plausible lengths, we synthesised five different 8-mer peptide libraries (Figure 1). Their compositions resemble either the contemporary amino acid alphabet ("19F", with the exclusion of cysteine due to the Fmoc-based peptide synthesis restrictions) or prebiotically plausible[23] amino acid alphabets, previously studied for their biophysical properties [26]: Specifically, the "10E" library consists of ten early canonical AAs; the "10U" library includes unbranched prebiotically available analogues replacing the branched residues in 10E; and the "11D" library expands 10E by adding diaminobutyric acid (DAB), a prebiotically available basic amino acid. Finally, the "11R" library includes arginine to assess the potential functional impact of a

contemporary positively charged residue on prebiotic evolution (Supplementary Figure 1). Although not typically detected in meteorites and atmospheric discharge experiments, plausibility of arginine prebiotic synthesis has been proposed from the cyanosulfidic protometabolism [47].

We tested how peptide libraries of different amino acid compositions interact with mineral and vesicle surfaces. Decanoic acid and decanol (DA:DOH) vesicles were selected as a prebiotically plausible vesicle system, as reported in previous studies [20,38]. The mineral fluorapatite was selected due to its abundance and prebiotic availability, as well as being a debated, yet potentially abundant source of phosphate in prebiotic chemistry [48,49]. Fluorapatite is more stable than hydroxyapatite and is commonly present in geological contexts on the Earth and Mars [50,51]. Peptide interactions were studied by incubation with DA:DOH vesicles or fluorapatite, followed by filtration for vesicle study, and centrifugation and release of bound peptides for fluorapatite. Resulting batches were then submitted to amino acid analysis.

Every peptide library screened exhibited binding propensity towards fluorapatite, with peptides containing "late" canonical amino acids (cAAs) showing higher binding capacity, as indicated by amino acid analysis experiments (Figure 2, B). Fluorapatite used in our experiments was sintered at temperature similar to that on prebiotic Earth (700 ℃), suggesting similar peptide-binding capacity of fluorapatite [52].

We then inquired into the specific changes of amino acid distribution of peptides bound to the fluorapatite surface to probe potential binding selectivity. Aspartate and glutamate were enriched in the peptides bound to fluorapatite across all libraries (Supplementary figure 2), consistent with their known affinity for apatite through coordination to calcium ions [53,54]. This enrichment happened even in libraries 19F and 11R, where the acidic residues were less abundant due to the presence of positively charged residues.

Next, we evaluated the binding propensity of peptide libraries to DA:DOH vesicles. We first confirmed the presence of vesicles using transmission electron microscopy complementary to fluorescent imaging (Supplementary figure 3). Upon incubation with vesicles, peptide concentrations varied depending on amino acid composition (Figure 2, C). Amicon Ultra-4 3K centrifugal filters have been used to separate the vesicle-bound and unbound peptides as reported in previous studies [20,55]. Nevertheless, we observed considerable binding of peptides to the filter itself and therefore only relative comparisons between the different libraries could be drawn with confidence. As such, we find that 10E and 10U libraries have ~80 % higher peptide concentration in the unbound phase than libraries with positively charged amino acids (19F, 11R and 11D), suggesting that positively charged amino acids might play a role in peptide-vesicle binding association, in alignment with previous reports on basic amino acid behaviour [13,38,42,56]. Interestingly, the 11D library (containing DAB) displayed a similar degree of vesicle binding as the 11R library (containing arginine), suggesting that DAB may modulate peptide binding to fatty acid vesicles, despite its weak mineral interaction. However, in the search of specific residues that would modulate binding to vesicles, we do not find substantial changes in amino acid distribution of peptides filtered from vesicle solution (Supplementary figure 4).

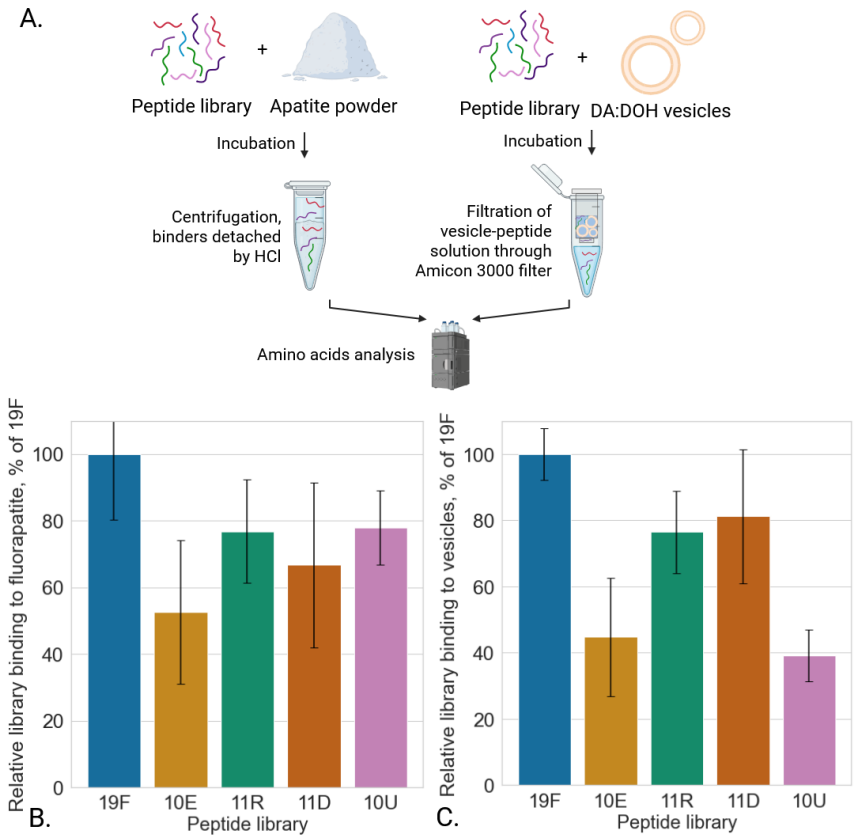

Figure 2. Peptide libraries association with prebiotic surfaces. A. Outline of experimental pipeline for establishing maximum adsorption of peptide libraries to fluorapatite and DA:DOH vesicles. Since it is impossible to centrifuge fatty acids down and since alcohols interfere with absorbance at 220 nm, HPLC was used to establish reduction in relative peptide concentration for both setups. B. Drop in relative peptide concentration as derived from amino acid analysis upon incubation with fluorapatite. Libraries with canonical positively charged amino acids show higher fluorapatite binding. Error bars – standard deviation from quadruplicates. C. Drop in relative peptide concentration upon incubation with DA:DOH vesicles and filtering through Amicon Ultra-4 3K centrifugal filter, as derived from amino acid analysis. Peptide libraries with positively charged amino acids show higher drop in relative concentration. Error bars – standard deviation from hexaplicates.

Inclusion of Arg in peptides enables phosphate release from apatite

Given that prebiotically plausible peptides bind to fluorapatite, we asked whether their binding could impact phosphate release from the mineral. We employed the molybdenum blue assay (Figure 3, A) and calibrated phosphate release against a standard curve (Supplementary figure 5). While Asp and Glu are crucial for fluorapatite binding, inclusion of Arg in peptide libraries seems to nearly double the amount of phosphate released (Figure 3, B). Increase in phosphate release upon 11R library binding can be attributed to by-chance acidic residues (Asp and Glu) coordinating with calcium ions, and Arg residues interacting with phosphate, catalysing the release reaction. The 19F library also enhances phosphate release, albeit to a lesser extent that 11R library. The 11D library (containing DAB instead of Arg) did not produce comparable effects, possibly due to DAB's shorter size and previously reported reduced secondary structure stability of the 11D library [26].

We performed this assay in both neutral and acidic pH and found that acidic pH on its own induces phosphate release from apatite, in line with a recent study [57]. All peptide libraries' binding induces

the release further, from a 6 µg in control conditions at pH 5.5, 25 °C to 8.3 µg and up to 12.7 µg (10E library and 11R library, respectively) of phosphate per 10 mg of fluorapatite (Figure 3). The acidic pH of 5.5 that we used is higher than the cutoff of pH 4 of efficient phosphate dissolution [57], and thus we hypothesize that peptides could have helped catalyse this reaction in a pH range closer to neutral.

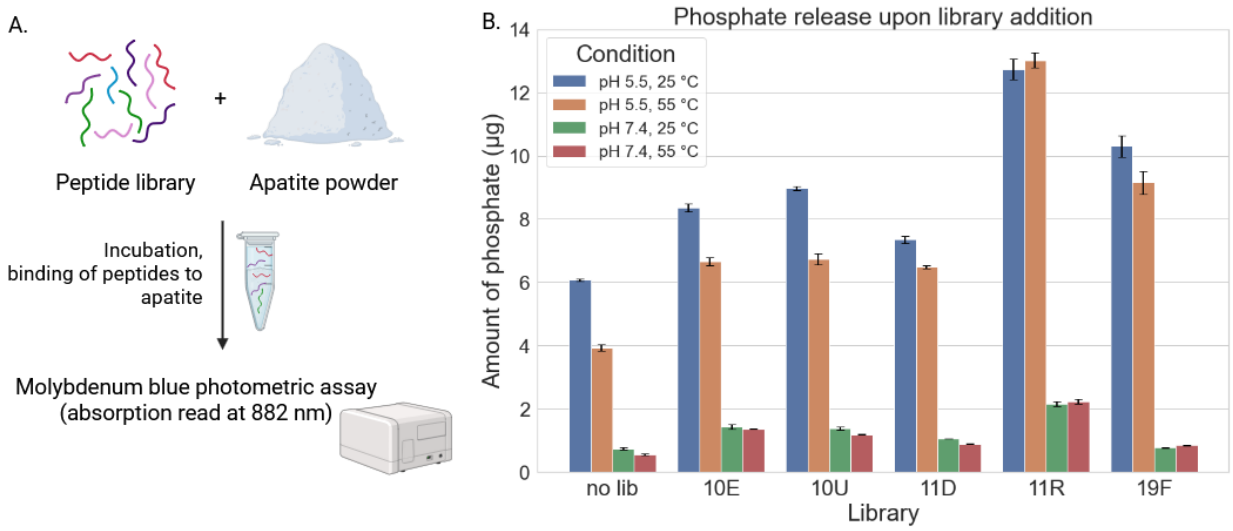

Figure 3. A. Outline of experimental workflow for establishing the amount of phosphate released from fluorapatite upon different pH, temperature and peptide library presence conditions. We used molybdenum blue photometric assay [58] in order to establish the amount of $H_2PO_4^{2-}$ in the sample. B. Phosphate release from fluorapatite, as measured after the addition of each peptide library under different pH and temperature. Error bars - standard deviations from triplicates.

Peptide libraries affect vesicle stability and abundance

We explored whether there is composition-dependent impact of peptide libraries on prebiotically plausible vesicles. The Hadean ocean, in which life is hypothesized to have emerged [59], probably had a significant salt content [60]. Both NaCl and divalent cations are necessary for life, yet both were reported to collapse and flocculate (aggregate) prebiotically plausible monogenic vesicles, although it should be noted that this effect would be likely alleviated in prebiotic environment by the intrinsically high heterogeneity of amphiphilic membrane constituents [20,55,61]. Previous reports indicate protective effects of selected amino acids and di- and tri-peptides against salt-induced flocculation [38], yet, to the best of our knowledge, no research on longer and more compositionally diverse peptides was conducted in a context of prebiotic evolution. We therefore measured changes in vesicle abundance and stability in presence of peptide libraries with and without addition of NaCl and $MgCl_2$ by spinning-disc fluorescent microscopy. This was accompanied by measurements of optical density at 490 nm (OD_{490}), which was reported to correlate with the level of multilamellarity and flocculation [20,55].

We observe that the effects of peptide libraries on vesicle stability are composition-dependent. Except 19F library, all libraries reduce OD_{490}, indicating potential loss of membranes. 10E library, which showed minimal vesicle binding, reduced vesicular stability the most, as indicated by the reduction in OD_{490} (~70 % of control) and the collapse of vesicles into previously reported [20] punctate

structures upon addition of $MgCl_2$ (Figure 4). The destabilization may originate from increased osmolarity or disruption of hydrogen bonding networks. The 10U library showed similar but less pronounced effects, possibly due to the longer chain length of unbranched residues like norvaline and norleucine facilitating fatty acid packing. Neither 10E or 10U libraries mitigated vesicle flocculation upon addition of NaCl. In contrast, 11R and 11D libraries protected vesicles from NaCl-induced flocculation, although the observed structures were not definitely vesicular. Overall, our findings suggest potentially disruptive effects of longer peptides composed of prebiotically available amino acids on fatty acid vesicles.

Nevertheless, inclusion of basic (11R, 11D) or unbranched (10U) amino acids improved peptide-membrane stability relative to 10E. This suggests that life could have benefited from transiently employing non-canonical amino acids (ncAAs) in peptide structures to negate potentially harmful effects of longer peptides on vesicles.

Inclusion of arginine seems to be beneficial in comparison to 10E composition for both mineral- and lipid-surface interactions. It aligns with a plethora of previous studies indicating uniqueness of guanidinium group [56,62], and further solidifies its position as a unique amino acid of utmost evolutionary importance.

The 19F library increased OD_{490} under all tested conditions and preserved vesicle integrity in both NaCl and $MgCl_2$ environments. Given its high binding affinity and low solubility [26], the inclusion of "late" amino acids appears to drive its stabilizing effects. These results suggest an evolutionary pressure to incorporate late cAAs to support membrane integrity in the face of potentially disruptive early peptides.

To test whether peptide-induced vesicle disruption could be attributed to altered membrane formation, we measured critical vesicle concentration (CVC), using pyrene fluorescence in vesicle-peptide dilutions. All libraries caused only a modest increase in CVC from ~1 mM to ~1.2-1.4 mM of DA:DOH. We find, then, that the changes in vesicle stability cannot be solely explained by an increase in critical vesicle concentration.

Our results expand on previous reports, where individual amino acids and short peptides typically had neutral or stabilizing effects on prebiotic vesicles [20,39,44,56]. We propose that the longer peptide length (8-mers) in our study could allow for secondary structure formation (≥4 residues for alpha-helices, ≥5 residues for beta-strands [63,64]), and these structures could be integrating into the fatty acid membranes with disruptive effects. Longer, hydrophobic peptides might arguably integrate into the bilayer, consistent with a prior simulation showing disruptive effects of Leu-Leu dimers [38].

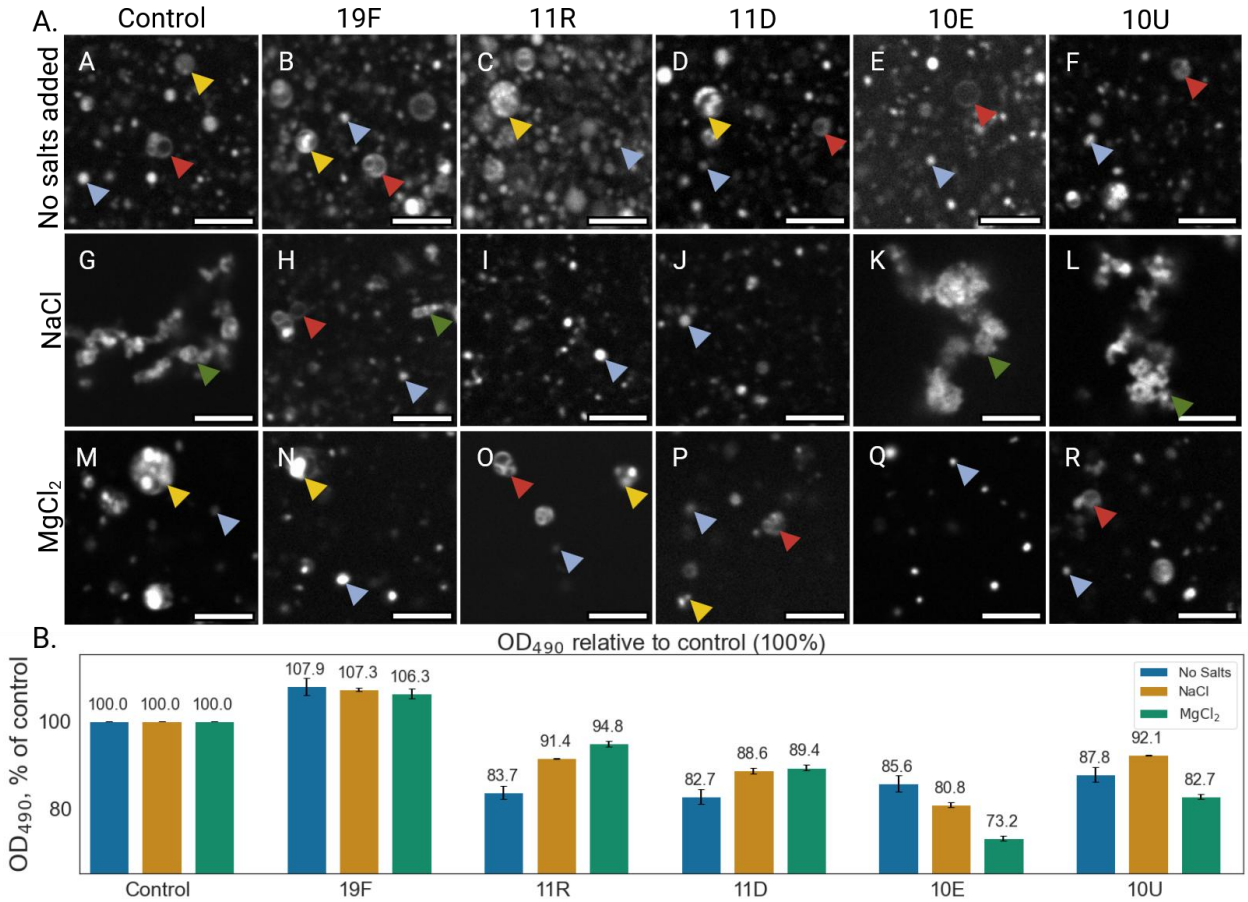

Figure 4. a. Microscopic images of DA:DOH (1:1) vesicles under different conditions. Vesicular flocculation can be observed upon addition of NaCl, as well as reduction in the number of visible particles upon addition of $MgCl_2$. Staining with Rhodamine 6G. Scale bar: 5 µm; Red arrow - unilamellar vesicle; yellow arrow - possible multilamellar vesicle; blue arrow - punctate structure; green arrow - flocs. b. Optical density at 490 nm for vesicles-peptide library samples ("19F", "11R", "10E", "11D", and "10U", peptide libraries added to free fatty acids before vesicle formation) under three conditions: no salts added, NaCl (363 mM final) and $MgCl_2$ (8.9 mM final). With the exception of 19F library, every peptide library screened reduces optical density of vesicles at 490 nm. Error bars represent the standard deviation from triplicates.

Addition of $MgCl_2$ or NaCl enhances peptide library co-localisation with DA:DOH vesicles

Peptide co-localisation with prebiotic vesicles is poorly understood [38]. Surface charge is of importance to the vesicle-peptide interactions and can mediate peptide's binding to membrane surfaces [65]. We used ζ-potential measurements to assess the correlation between the vesicle behaviour and their relative charge. We find that 38.5 mM DA:DOH vesicles have a ζ -potential of -54.6±2.65 mV; in presence of NaCl and $MgCl_2$, the ζ -potential drops to -17.6±9.2 mV and -32.6±2.45 mV, respectively (Supplementary table 1). This likely contributes to vesicle flocculation: since vesicles' surface charge is negated by the presence of ions, they are subject to much less repelling, and, as such, tend to flocculate. Addition of peptide libraries only slightly reduces the ζ -potential (for example, to -49.6±4 mV and -46.2±2.8 mV for 11R and 10E libraries, respectively), so we argue that ζ -potential might not be a decisive factor mediating peptide libraries effects on vesicles, but that the reduction of ζ -potential in the presence of salt and divalent cations might ease peptide's association with fatty acids.

To visualize peptide-vesicle co-localisation, we labeled peptide libraries with canonical amino acid alphabet (19F, 11R, and 10E) with TAMRA and imaged them using spinning-disc microscopy alongside DiD-stained vesicles. We observed that even peptide libraries with weak vesicle association in prior filtration assays exhibited marked co-localization with vesicle membranes upon the addition of NaCl and Mg^{2+} (Figure 5), possibly due to the above-mentioned reduction in vesicles' ζ-potential. We propose that the neutralisation of repelling forces on both membranes and peptides by NaCl and Mg^{2+} increases co-localisation of peptides and fatty acids, and that Mg^{2+} can also act as a "bridging" agent between these molecules. We argue that this co-localisation of peptide libraries indicates potential association, binding or even membrane integration, as recently reported by molecular dynamics simulation [38].

Notably, we find visual co-localisation of peptide libraries with DA:DOH membranes if peptide libraries were added to free fatty acids prior vesicle formation; when added to pre-made vesicles, no observable co-localisation occurred between DA:DOH vesicles and 10E and 10R libraries. We suggest that peptide libraries could integrate into the forming membranes and potentially modulate membrane formation, as indicated by the relative changes in OD_{490} in earlier experiments. In contrast, peptides added to post-vesicles assembly could likely be repelled by the negative surface charge of vesicles.

Although DA:DOH vesicles were reported to allow the passage of molecules through the membrane [66], we did not find substantial accumulation of fluorescently labelled peptides in intravesicular lumen by microscopy if peptides were added to pre-made vesicles (Figure 5). We hypothesise that, due to their composition, at least 19F and 11R libraries could potentially permeate through the fatty acid membranes, but, due to the short time period in which the measurements were conducted upon the formation of vesicles (~5-10 minutes), the membrane permeability should not have been substantial enough to observe.

Overall, our results suggest that peptide localisation relative to fatty acids is of high importance to the emergent effects. Given that peptides, free fatty acids and self-assembled vesicles could conceivably coexist in the same prebiotic environment [67,68], we argue that there could have been a mix of both integration and surface binding of peptides into early organic interfaces.

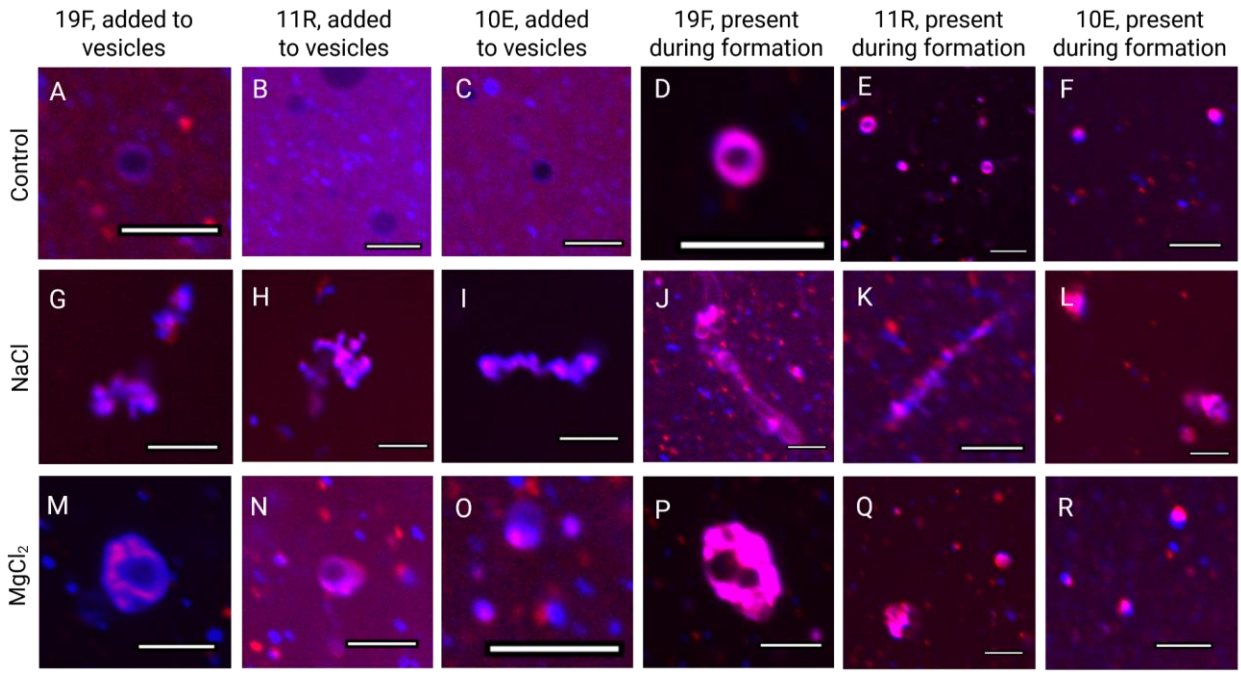

Figure 5. Fluorescence microscopy images of vesicles with peptide libraries either added to already formed vesicles (columns A-C, G-I, M-O) or present during vesicle formation (columns D-F, J-L, P-R) under three conditions: Control (top row), 363 mM NaCl (middle row), and 9.1 mM $MgCl_2$ (bottom row). Peptide libraries (19F, 11R, and 10E) are stained with TAMRA (red channel), while lipids are stained with DiD (blue channel). Addition of NaCl (middle row) induces vesicle aggregation and peptide co-localisation with the membranes (columns G-I), with similar, yet less pronounced effects upon addition of $MgCl_2$ (columns M-O). Peptide libraries present in the solution before vesicle formation (columns D-F, J-L, P-R) consistently exhibit more stable co-localisation with vesicular membranes across conditions. Scale bars represent 5 µm.

Conclusions

As plausible predecessors of proteins, peptides likely helped to shape the path between the chemical networks provided by geochemistry and life's biochemistry as we know it. Besides their structural and catalytic potential, the interaction of peptides with other prebiotically abundant species could have driven the chemical evolution of the amino acid alphabet towards its biological repertoire. In this study, we explored the effects of peptide compositions on their propensity to interact with vesicles and mineral surfaces using vast peptide libraries.

The prebiotically available pool of amino acids allowed peptides to interact favourably with mineral surfaces, yet it appears that there was a need for the expansion of the amino acid alphabet in order to favour lipid-peptide interactions and reduce their membrane-destabilising effects.

Acknowledgements

This work was supported by a Research Grant from HFSP https://doi.org/10.52044/HFSP.RGEC272023.pc.gr.168579. M.M. and I.C. acknowledge support by the project the "Grant Schemes at CU" (reg. no. CZ.02.2.69/0.0/0.0/19_073/0016935), project no. START/SCI/148. K.H., M.M., and I.C. acknowledge CMS CF Biophysical techniques of CIISB, Instruct-CZ Centre, supported by MEYS CR Infrastructure project LM2018127 and European Regional Development Fund-Project, "UP CIISB" (No. CZ.02.1.01/0.0/0.0/18_046/ 0015974). SFJ acknowledges support from European Research Council (ERC) under the European Union's Horizon Europe research and innovation programme (grant agreement No 1101114969) and Science Foundation Ireland (SFI Pathway award 22/PATH-S/10692).

References

[1] D. Deamer, J. P. Dworkin, S. A. Sandford, M. P. Bernstein, L. J. Allamandola, *Astrobiology* **2002**, *2*, 371–381.

[2] D. Toparlak, M. Karki, V. Egas Ortuno, R. Krishnamurthy, S. S. Mansy, *Small* **2020**, *16*, 1–8.

[3] C. L. Apel, D. W. Deamer, M. N. Mautner, *Biochimica et Biophysica Acta - Biomembranes* **2002**, *1559*, 1–9.

[4] K. Morigaki, P. Walde, *Current Opinion in Colloid and Interface Science* **2007**, *12*, 75–80.

[5] J. G. Lawless, G. U. Yuen, *Nature* **1979**, *282*, 396–398.

[6] D. W. Deamer, R. M. Pashley, *Origins of Life and Evolution of the Biosphere* **1989**, *19*, 21–38.

[7] J. F. Lambert, *Origins of Life and Evolution of Biospheres* **2008**, *38*, 211–242.

[8] E. Biondi, S. Branciamore, M. C. Maurel, E. Gallori, *BMC Evolutionary Biology* **2007**, *7*, 1–7.

[9] A. J. A. Aquino, D. Tunega, M. H. Gerzabek, H. Lischka, *Journal of Physical Chemistry B* **2004**, *108*, 10120–10130.

[10] W. H. Yu, N. Li, D. S. Tong, C. H. Zhou, C. X. Lin, C. Y. Xu, *Applied Clay Science* **2013**, *80–81*, 443–452.

[11] A. Rimola, D. Costa, M. Sodupe, J. F. Lambert, P. Ugliengo, *Chemical Reviews* **2013**, *113*, 4216–4313.

[12] C. Mayer, U. Schreiber, M. J. Dávila, O. J. Schmitz, A. Bronja, M. Meyer, J. Klein, S. W. Meckelmann, *Life* **2018**, *8*, DOI 10.3390/life8020016.

[13] W. Kwiatkowski, R. Bomba, P. Afanasyev, D. Boehringer, R. Riek, J. Greenwald, *Angewandte Chemie - International Edition* **2021**, *60*, 5561–5568.

[14] C. Bonfio, L. Valer, S. Scintilla, S. Shah, D. J. Evans, L. Jin, J. W. Szostak, D. D. Sasselov, J. D. Sutherland, S. S. Mansy, *Nat Chem.* **2018**, *9*, 1229–1234.

[15] C. S. Foden, S. Islam, C. Fernández-García, L. Maugeri, T. D. Sheppard, M. W. Powner, *Science* **2020**, *370*, 865–869.

[16] B. K. B. Muchowska, J. Moran, *Science* **2020**, *370*, 767–769.

[17] P. van der Gulik, S. Massar, D. Gilis, H. Buhrman, M. Rooman, *Journal of Theoretical Biology* **2009**, *261*, 531–539.

[18] M. Gorlero, R. Wieczorek, K. Adamala, A. Giorgi, M. E. Schininà, P. Stano, P. L. Luisi, *FEBS Letters* **2009**, *583*, 153–156.

[19] K. Kon, H. Takai, Y. Kohari, M. Murata, *Catalysts* **2019**, *9*, 33–36.

[20] C. E. Cornell, R. A. Black, M. Xue, H. E. Litz, A. Ramsay, M. Gordon, A. Mileant, Z. R. Cohen, J. A. Williams, K. K. Lee, G. P. Drobny, S. L. Keller, *Proceedings of the National Academy of Sciences of the United States of America* **2019**, *116*, 17239–17244.

[21] P. Dalai, N. Sahai, *Trends in Biochemical Sciences* **2019**, *44*, 331–341.

[22] E. N. Trifonov, *Gene* **2000**, *261*, 139–151.

[23] P. G. Higgs, R. E. Pudritz, *Astrobiology* **2009**, *9*, 483–490.

[24] H. J. Cleaves, *Journal of Theoretical Biology* **2010**, *263*, 490–498.

[25] C. Mayer-Bacon, M. Meringer, R. Havel, J. C. Aponte, S. Freeland, *Journal of Molecular Evolution* **2022**, *90*, 307–323.

[26] M. Makarov, A. C. S. Rocha, R. Krystufek, I. Cherepashuk, V. Dzmitruk, T. Charnavets, A. M. Faustino, M. Lebl, K. Fujishima, S. D. Fried, K. Hlouchova, *Journal of the American Chemical Society* **2023**, *145*, 5320–5329.

[27] V. Tretyachenko, T. Neuwirthová, *Open Biology* **2022**, *12*, DOI https://doi.org/10.1098/rsob.220040.

[28] L. M. Longo, D. Despotović, O. Weil-Ktorza, M. J. Walker, J. Jabłońska, Y. Fridmann-Sirkis, G. Varani, N. Metanis, D. S. Tawfik, *Proceedings of the National Academy of Sciences of the United States of America* **2020**, *117*, 15731–15739.
[29] A. C. Sanchez-Rocha, M. Makarov, L. Pravda, M. Novotný, K. Hlouchová, *eLife* **2024**, *13*, RP94174–RP94174.
[30] K. H. Valerio Guido Giacobelli, Kosuke Fujishima, Martin Lepsik, Vyacheslav Tretyachenko, Tereza Kadava, Lucie Bednarova, Petr Novak, *bioRxiv* **2021**, DOI https://doi.org/10.1101/2021.08.01.454623.
[31] K. Hlouchová, *Accounts of Chemical Research* **2024**, *57*, 2027–2037.
[32] N. Lane, J. F. Allen, W. Martin, *BioEssays* **2010**, *32*, 271–280.
[33] L. M. Longo, M. Blaber, *Archives of Biochemistry and Biophysics* **2012**, *526*, 16–21.
[34] V. Erastova, M. T. Degiacomi, D. G. Fraser, H. C. Greenwell, *Nature Communications* **2017**, *8*, 1–9.
[35] R. A. Peckauskas, I. Pullman, J. D. Termine, *Biopolymers* **1977**, *16*, 199–206.
[36] M. E. Bolander, M. F. Young, L. W. Fisher, Y. Yamada, J. D. Termine, *Proceedings of the National Academy of Sciences of the United States of America* **1988**, *85*, 2919–2923.
[37] D. B. DeOliveira, R. A. Laursen, *Journal of the American Chemical Society* **1997**, *119*, 10627–10631.
[38] Z. R. Cohen, Z. R. Todd, L. Maibaum, D. C. Catling, R. A. Black, *Langmuir* **2024**, *40*, 8971–8980.
[39] M. Xue, R. A. Black, Z. R. Cohen, A. Roehrich, G. P. Drobny, S. L. Keller, *Journal of Physical Chemistry B* **2021**, *125*, 7933–7939.
[40] S. Murillo-Sánchez, D. Beaufils, J. M. González Mañas, R. Pascal, K. Ruiz-Mirazo, *Chemical Science* **2016**, *7*, 3406–3413.
[41] T. Hitz, P. L. Luisi, *Biopolymers - Peptide Science Section* **2000**, *55*, 381–390.
[42] N. P. Kamat, S. Tobé, I. T. Hill, J. W. Szostak, *Angewandte Chemie - International Edition* **2015**, *54*, 11735–11739.
[43] M. T. Gordon, R. A. Black, C. Cornell, J. A. Williams, K. K. Lee, S. L. Keller, *Biophysical Journal* **2016**, *110*, 85a–85a.
[44] M. P. Joshi, A. A. Sawant, S. Rajamani, *Chem. Sci.* **2021**, *12*, 2970–2978.
[45] M. P. Joshi, A. Uday, S. Rajamani, *Commun Chem* **2022**, *5*, 147.
[46] M. Preiner, S. Asche, S. Becker, H. C. Betts, A. Boniface, E. Camprubi, K. Chandru, V. Erastova, S. G. Garg, N. Khawaja, G. Kostyrka, R. Machné, G. Moggioli, K. B. Muchowska, S. Neukirchen, B. Peter, E. Pichlhöfer, Á. Radványi, D. Rossetto, A. Salditt, N. M. Schmelling, F. L. Sousa, F. D. K. Tria, D. Vörös, J. C. Xavier, *Life* **2020**, *10*, DOI 10.3390/life10030020.
[47] B. H. Patel, C. Percivalle, D. J. Ritson, C. D. Duffy, J. D. Sutherland, *Nature Chemistry* **2015**, *7*, 301–307.
[48] A. Paytan, K. McLaughlin, *Chemical Reviews* **2007**, *107*, 563–576.
[49] C. R. Walton, S. Ewens, J. D. Coates, R. E. Blake, N. J. Planavsky, C. Reinhard, P. Ju, J. Hao, M. A. Pasek, *Nature Geoscience* **2023**, *16*, 399–409.
[50] E. M. Hausrath, O. Tschauner, *Astrobiology* **2013**, *13*, 1049–1064.
[51] M. Martínez, C. K. Shearer, A. J. Brearley, *Meteorit & Planetary Scien* **2023**, *58*, 1229–1245.
[52] S. Jeyapalina, E. Hillas, J. P. Beck, J. Agarwal, J. Shea, *Journal of the Mechanical Behavior of Biomedical Materials* **2022**, *125*, 104950.
[53] M. Tavafoghi, M. Cerruti, *J. R. Soc. Interface.* **2016**, *13*, 20160462.
[54] S. E. Hoff, J. Liu, H. Heinz, *Journal of Colloid and Interface Science* **2022**, *605*, 685–700.
[55] R. A. Black, M. C. Blosser, B. L. Stottrup, R. Tavakley, D. W. Deamer, S. L. Keller, *Proceedings of the National Academy of Sciences of the United States of America* **2013**, *110*, 13272–13276.

[56] D. J. Mitchell, L. Steinman, D. T. Kim, C. G. Fathman, J. B. Rothbard, *Journal of Peptide Research* **2000**, *56*, 318–325.
[57] T. Matreux, A. Schmid, M. Rappold, D. Weller, A. Z. Çalışkanoğlu, K. R. Moore, T. Bosak, D. B. Dingwell, K. Karaghiosoff, F. Guyot, B. Scheu, D. Braun, C. B. Mast, *Nature Communications* **2025**, *16*, DOI 10.1038/s41467-025-57110-3.
[58] J. Murphy, J. P. Riley, *Analytica Chimica Acta* **1962**, *27*, 31–36.
[59] E. E. Stüeken, R. E. Anderson, J. S. Bowman, W. J. Brazelton, J. Colangelo-Lillis, A. D. Goldman, S. M. Som, J. A. Baross, *Geobiology* **2013**, *11*, 101–126.
[60] L. P. Knauth, *Palaeogeography, Palaeoclimatology, Palaeoecology* **2005**, *219*, 53–69.
[61] S. F. Jordan, H. Rammu, I. N. Zheludev, A. M. Hartley, A. Maréchal, N. Lane, *Nat Ecol Evol* **2019**, *3*, 1705–1714.
[62] M. Vazdar, J. Heyda, P. E. Mason, G. Tesei, C. Allolio, M. Lund, P. Jungwirth, *Acc. Chem. Res.* **2018**, *51*, 1455–1464.
[63] S. Mondal, M. Varenik, D. N. Bloch, Y. Atsmon-Raz, G. Jacoby, L. Adler-Abramovich, L. J. W. Shimon, R. Beck, Y. Miller, O. Regev, E. Gazit, *Nat Commun* **2017**, *8*, 14018.
[64] H. E. Stanger, F. A. Syud, J. F. Espinosa, I. Giriat, T. Muir, S. H. Gellman, *Proc. Natl. Acad. Sci. U.S.A.* **2001**, *98*, 12015–12020.
[65] I. A. Chen, J. W. Szostak, *Biophysical Journal* **2004**, *87*, 988–998.
[66] I. Budin, J. W. Szostak, *Proceedings of the National Academy of Sciences of the United States of America* **2011**, *108*, 5249–5254.
[67] T. M. Mccollom, G. Ritter, B. R. T. Simoneit, *Origins of Life and Evolution of the Biosphere* **1999**, *29*, 153–166.
[68] E. I. Imai, H. Honda, K. Hatori, A. Brack, K. Matsuno, *Science* **1999**, *283*, 831–833.

Methodology

Chemicals

For the solid-phase synthesis of combinatorial peptide libraries, Fmoc-Rink Amide AM resin (100-200 mesh, 0.62 mmol/g loading) and Fmoc-protected amino acids were purchased from Iris Biotech (Germany). N,N'-dimethylformamide (DMF) was purchased from Carl Roth (Germany), dichloromethane and diethyl ether were purchased from PENTA (Czech Republic). Ceramic hydroxyapatite and fluorapatite (type II, 40 µm particle size) were purchased from Bio-Rad (USA). All other chemicals were purchased from Sigma Aldrich (USA). For experiments related to vesicle interactions, Rhodamine 6G, DA were purchased from ThermoFisher Scientific (USA), and DOH was purchased from Sigma Aldrich.

Chemical synthesis of combinatorial peptide libraries

8-mer combinatorial peptide libraries were prepared manually using Fmoc-based solid-phase synthesis. Synthesis of the peptide mixtures was accomplished by coupling Fmoc-protected amino acids individually to the equal aliquots of the solid support that were merged after coupling (split and mix approach). Prior to synthesis, Fmoc-amino acid/Oxyma Pure stock solutions were prepared by simultaneously dissolving Fmoc-amino acids and Oxyma Pure to the final concentrations of 350 mM and 425 mM in DMF, respectively. 500 mg of Rink Amide AM resin (0.31 mmol) was swelled in 20 ml of DMF for 1 h and subsequently deprotected by incubation with 15 ml of 20 % (v/v) piperidine in DMF for 1 h at room temperature. The resin was washed four times with 10 ml of DMF, thoroughly resuspended in 10 ml of DMF and split into equal aliquots, depending on the number of amino acids (10 for “10E”, 11 for “10U”, “11R”, “11D”, and 19 for “19F” peptide libraries). For the synthesis of “10E” peptide library, 1.1 ml of Fmoc-amino acid/Oxyma Pure solutions and 64 µl of N,N'-diisopropylcarbodiimide were added to the resin aliquots, and the reaction mixture was incubated overnight at room temperature. The amounts of Fmoc-amino acid/Oxyma Pure solution and N,N'-diisopropylcarbodiimide used for coupling were scaled down for a higher number of amino acids (resin aliquots). Following the coupling, the resin aliquots were merged, washed five times with 10 ml of DMF and deprotected by incubation with 15 ml of 20% (v/v) piperidine in DMF for 1 hour at room temperature. The amino acid coupling and deprotection steps were performed eight times. All separation and washing steps were performed using 15 ml polypropylenesyringes fittedwith polypropylene frits. After the final coupling/deprotection step, the resin was washed five times with 10 ml of dichloromethane and dried *in vacuo*. The peptide mixture was cleaved off the dried resin by incubation with 10 ml of trifluoroacetic acid-triisopropylsilane-water (95:2.5:2.5, v/v) mixture for 2 hours at room temperature. The resin was filtered off, and the peptide mixture was precipitated with 150 ml of diethyl ether cooled down to 4 ℃ and submerged in liquid nitrogen for 10 min to maximize precipitation. The peptide mixture was subsequently centrifuged at 5000× g for 5 min at 4 ℃, and the peptide pellet was collected and lyophilized three times with 1 mM HCl overnight.

Additionally, 19F, 10E, and 11R libraries were synthesized with the inclusion of the TAMRA fluorescent dye for peptide co-localisation assays. Labelling was performed by overnight treatment with 3 eq. of 5(6)-carboxytetramethylrhodamine, 3.75 eq. Oxyma Pure and 3.75 eq. N,N'-diisopropylcarbodiimide in DMF after the final coupling/deprotection step.

Quality control of combinatorial peptide libraries

The molecular weight distributions of 8-mer combinatorial peptide libraries were confirmed by mass spectrometry using UltrafleXtreme MALDI-TOF/TOF mass spectrometer (Bruker Daltonics, Germany) according to the standard procedure. Prior to the MALDI-TOF analysis, peptide libraries were dissolved in acetonitrile:water (50:50, v/v) mixture and mixed with 2,5-dihydroxybenzoic acid (DHB) that was used as a matrix.

The amino acid composition of 8-mer combinatorial peptide libraries was estimated by HPLC amino acid analysis performed on Agilent 1260 HPLC system (Agilent Technologies, Germany) equipped with a fluorescence detector using automated ninhydrin derivatization. Prior to the HPLC amino acid analysis, the library samples were hydrolyzed in 6 M HCl at 110 °C for 20 h with the hydrolysate evaporated and reconstituted with 0.1 M HCl.

HPLC amino acid and mass spectrometry analyses of mineral binders from 8-mer combinatorial peptide libraries

50 mg of fluorapatite was gently rotated with 1 ml of 1 mg/ml peptide library solution in HMA buffer (20 mM HEPES, 20 mM MES, 20 mM sodium acetate, pH 7.4) for 6 hours at room temperature. The mixture was centrifuged at 15000× g for 3 min at room temperature to separate apatite from the peptide library solution, and the supernatant was subsequently discarded. The apatite was resuspended in 0.5 ml of HMA buffer (pH 7.4), incubated for 3 min at room temperature and centrifuged at 15000× g for 3 min. The washing step was repeated four times. The bound peptides were subsequently released from apatite by overnight incubation with 220 µl of 50 mM HCl at room temperature. Following the incubation, the mixture was centrifuged at 15000× g for 3 min, and 100 µl of supernatant was submitted to MALDI-TOF or HPLC amino acid analyses. Mass spectrometry was performed once, an HPLC analysis was performed twice.

Phosphate release by 8-mer combinatorial peptide libraries

Solubilization of fluorapatite by combinatorial peptide libraries at two different pH (5.5 or 7.4) and temperature (25 or 55 ℃) conditions was estimated by molybdenum blue spectrophotometric assay [58]. Prior to analysis, molybdenum blue reagent was freshly prepared by mixing 2.5 M sulphuric acid, ammonium molybdate (40 g/l), 0.1 M ascorbic acid, and potassium antimonyl tartrate (1 mg Sb/ml) in 10:3:6:1 (v/v) ratio. 10 mg of apatite was gently rotated with 0.5 ml of 1 mg/ml peptide library solution in HMA buffer for 21 hours. The mixture was centrifuged at maximum speed (21.300× g) for 20 min at 4 ℃ to separate apatite from the peptide library solution, and 350 µl of supernatant was transferred to a new tube. The supernatant was centrifuged again at maximum speed (21.300× g) for 20 min at 4 ℃ to remove any residual apatite, and 320 µl of supernatant was transferred to a new tube. 5 µl (for 25 ℃ incubation) or 75 µl (for 55 ℃ incubation) of supernatant was mixed with MilliQ water to adjust the volume to 150 µl in a 96-well plate, and 30 µl of molybdenum blue reagent was added to each well. The reaction mixture was incubated for 20 min at room temperature, and the absorbance at 882 nm was measured using Infinite M Plex plate reader (TECAN, Switzerland). The amount of phosphate ions in the supernatant was quantified from the standard curve established using 2-fold serial dilutions of KH_2PO_4 solution in MilliQ water. The measurement was performed in technical fourplicates. The analysis was performed once.

Preparation of stock decanoic acid:decanol (DA:DOH) vesicle solution

Decanoic acid (DA) and decanol (DOH) offer relative stability for vesicle experimentation and were observed in meteorite materials [6]. All solutions were pre-warmed to 70 ℃ using a water bath. DA was dissolved in 340 volumes of acetate-phosphate-borate buffer (ABP, pH 7.4) or 5 mg/mL peptide library solution in ABP (in experiments where peptide libraries were present in the lipid solution prior vesicle formation). The mixture was mixed vigorously for 30 seconds, followed by the addition of 180 mM NaOH to achieve a DA concentration of 53 mM. DOH was then added in an equimolar concentration to DA, and the solution was mixed vigorously for 60 seconds to allow vesicle formation. The pH was adjusted to 7.4 using HCl, resulting in a final concentration of 77 mM for both DA and DOH. The stock solution was then mixed vigorously for another 60 seconds and used in experiments downstream.

Preparation of peptide library solution for experimentation on DA:DOH vesicles

5 mg of peptide library was dissolved in ABP to a final concentration of 5 mg/ml. This solution upon mixing by pipetting was either added to DA (in experiments where peptide libraries were present in the lipid solution prior vesicle formation) or diluted with ABP to a concentration of 2 mg/ml. In such cases, these stock solutions were used in consequent experiments shortly upon mixing by pipetting to ensure uniform concentration and sedimentation of potential microaggregates.

Amino acid analysis of peptide libraries upon incubation with DA:DOH vesicles

150 µl of the DA:DOH vesicle stock solution was mixed with 150 µl of 2 mg/ml solution of peptide libraries in ABP ("vesicle incubation" condition) or ABP alone (negative control) and incubated at 25 ℃ with shaking at 1000 RPM, 2 mm orbit for 1 hour. Additionally, peptide libraries were incubated in the absence of vesicle stock solution (replaced with ABP) in parallel ("vesicle control" condition in order to elucidate peptide library binding to Amicon filter itself). 10 µl of the resulting solution was dried out and submitted to amino acid analysis ("unfiltered" condition), and other 250 µl of the were loaded into Amicon Ultra-4 3K centrifuge filters and centrifuged at 3000× g for 10 minutes. 10 µl of the flow-through from the Amicon centrifuge filters were also dried out and submitted to amino acid analysis ("filtered" condition). Amino acid analysis was performed on a Biochrom 30 amino acid analyzer. Results from the negative control were subtracted from the results, and both relative concentrations of individual amino acids and whole peptide library concentration were compared relatively within each condition. All experiments were conducted in hexaplicates.

Zeta-potential measurements

Measurements of zeta-potential of vesicle populations were conducted using Zetasizer Nano ZS90 (Malvern Panalytical) with DTS1070 cuvettes at standard manufacturer settings at 25 ℃. 350 µl of vesicle stock were mixed with 350 µl of either ABP or 2 mg/ml peptide library solution in ABP, and 70 µl of 4M NaCl or 100 mM $MgCl_2$ solutions were also added, depending on the experiment, to a final concentration of 363 and 8.9 mM, respectively. Experiments were conducted in technical triplicates.

Spinning-disc confocal microscopy

50 µl of stock vesicle solutions were mixed in a 1:1 ratio with 2 mg/mL solutions of peptide libraries in ABP buffer on Glass Bottom 18-Well µ-Slides (Ibidi, Germany). Rhodamine 6G (excitation peak at 561 nm) was added to a final concentration of 1 µM. For specific experiments, 10 µl of 4M NaCl solution was added to a final concentration of 363 mM or 10 µl of 100 mM $MgCl_2$ solution to a final

concentration of 9.1 mM. In alternative setups, 2 mg/ml of peptide library solution in ABP conjugated with TAMRA fluorescent dye (excitation at 561 nm) were mixed with their non-fluorescent counterparts (2 mg/ml in ABP) in a 1:50 ratio. In such instances, DiD fluorescent dye (excitation at 638 nm) was used for membrane imaging instead of Rhodamine 6G, which is has overlapping excitation range with TAMRA. Imaging was performed using a Nikon CSU-W1 spinning-disc confocal microscope with a 100× oil-immersion objective and a PRIME BSI camera (Teledyne Photometrics) at room temperature.

Transmission electron microscopy

100 µl of DA:DOH vesicle solution was diluted in 900 µl PBS buffer to a final concentration of 7.7 mM. Vesicle sample was then analysed in PBS buffer by negative staining. Parlodion-carbon-coated grids were floated on the top of 10 µl drop of the sample for 5 min. Then the grids were stained of 2% uranyl acetate, for 2 × 30 s and dried. The grids were examined with a JEOL JEM-2100 Plus electron microscope operated at 200 kV (JEOL Ltd., Japan).

Turbidity measurement

Turbidity measurements were conducted in 96-well plates on a microplate reader (Infinite M Plex, Tecan, Switzerland). Vesicle solutions were prepared in presence of peptide libraries with free fatty acids as outlined above. 10 µl of 4 M NaCl or 10 µl of 100 mM $MgCl_2$ solutions were added to final concentrations of 363 mM or 9.1 mM, respectively. OD_{490} measurement was then conducted in triplicates, and absorbance was compared against average vesicle sample absorbance at the absence of peptide libraries, which was put at 100% for every salt addition condition screened (control (no salts added), 363 mM NaCl or 9.1 mM $MgCl_2$).

Critical vesicle concentration measurement

Critical vesicle concentration (CVC) was established by preparing serial dilution of vesicle stock solution with or without peptide libraries (from 0.35 to 11.33 mM, 100 µl final sample volume in a 96-well plate), adding 2 µl of pyrene dye (1 mM stock solution in methanol) to final concentration of 5 µM and measuring fluorescence emission at 384 and 373 nm using Infinite M Plex microplate reader (Tecan, Switzerland) at 25 ℃. The 384/373 ratio curve was then plotted against vesicle concentration and the approximation of CVC was evaluated at the 1.15 384/373 ratio cutoff point.

Supplements

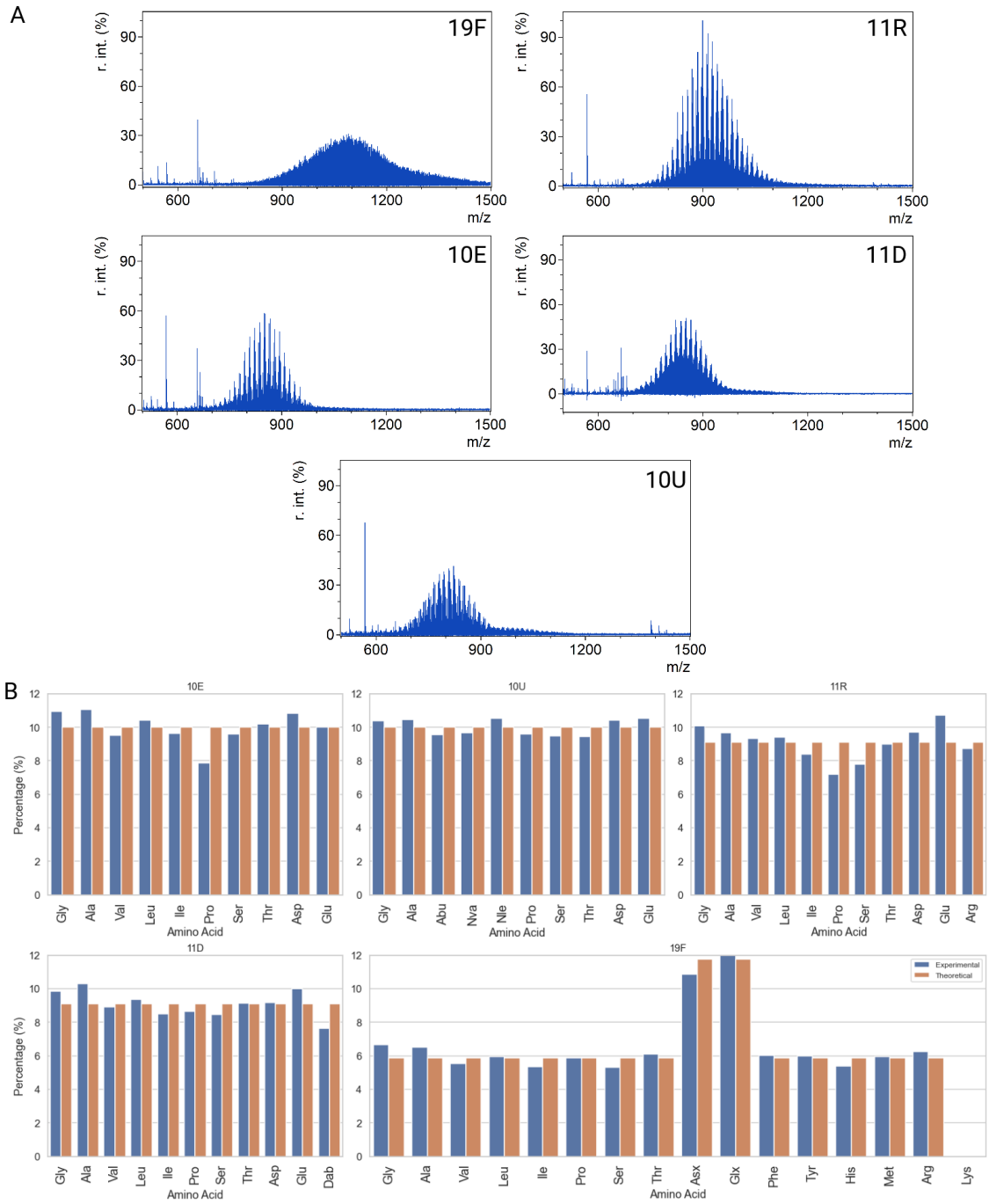

Supplementary figure 1. Matrix-assisted laser desorption/ionization (A) and HPLC amino acid analysis (B) of 8-mer random peptide libraries used in the current work, showing molecular size and amino acid distribution in a satisfactory range from theoretical ones. Since Asp and Glu overlap with Asn and Gln on HPLC graph, they are pulled together at the amino acid distribution graphs for 19F and labelled Asx and Glx, respectively.

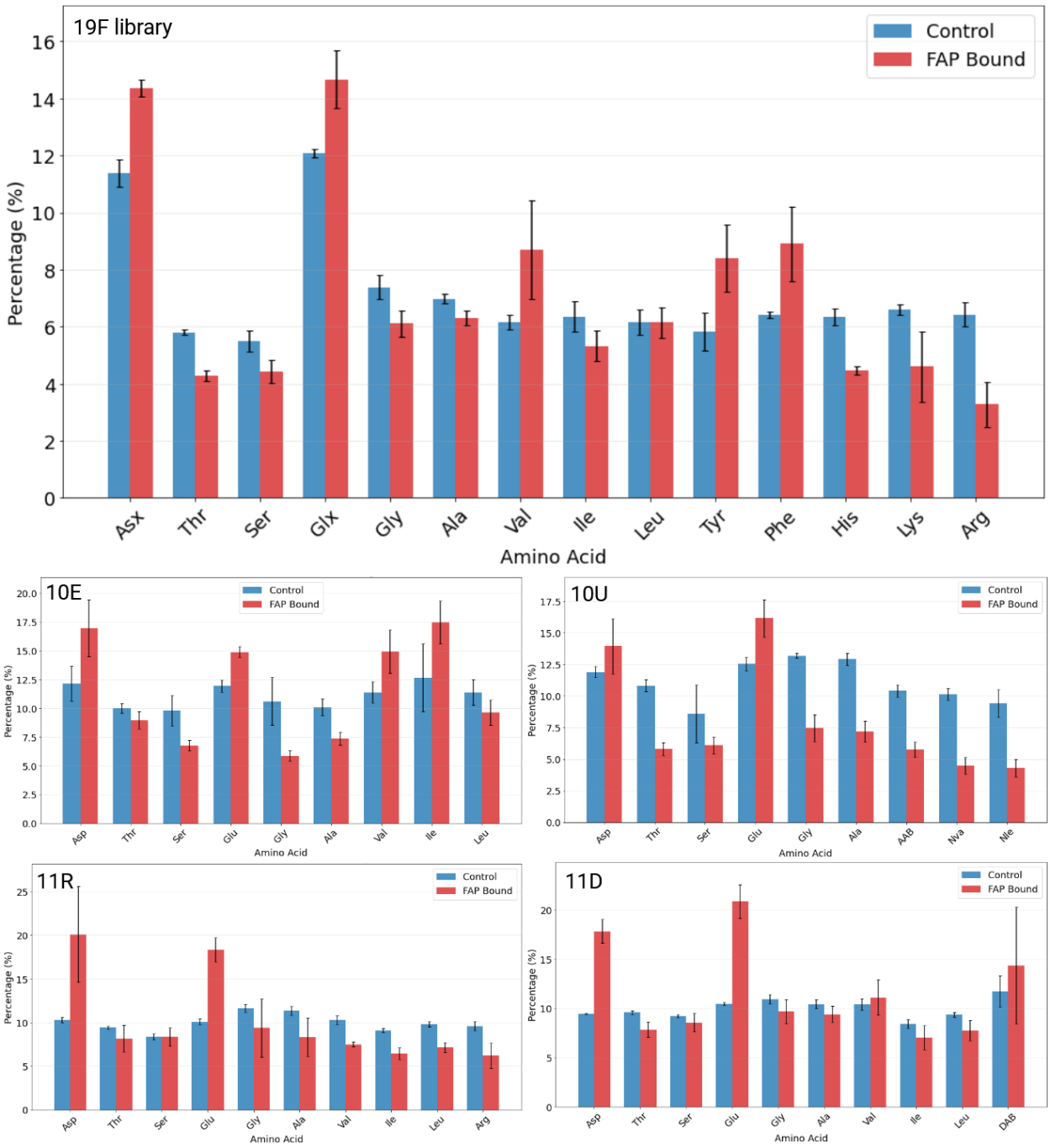

Supplementary figure 2. Amino acid distribution of random peptide libraries upon binding to fluorapatite. We find enrichment in aspartate and glutamate in the bound fraction of every screened library, indicating their potential binding mediation. Since Asp and Glu overlap with Asn and Gln on HPLC graph, they are pulled together at the amino acid distribution graphs for 19F and labelled Asx and Glx, respectively.

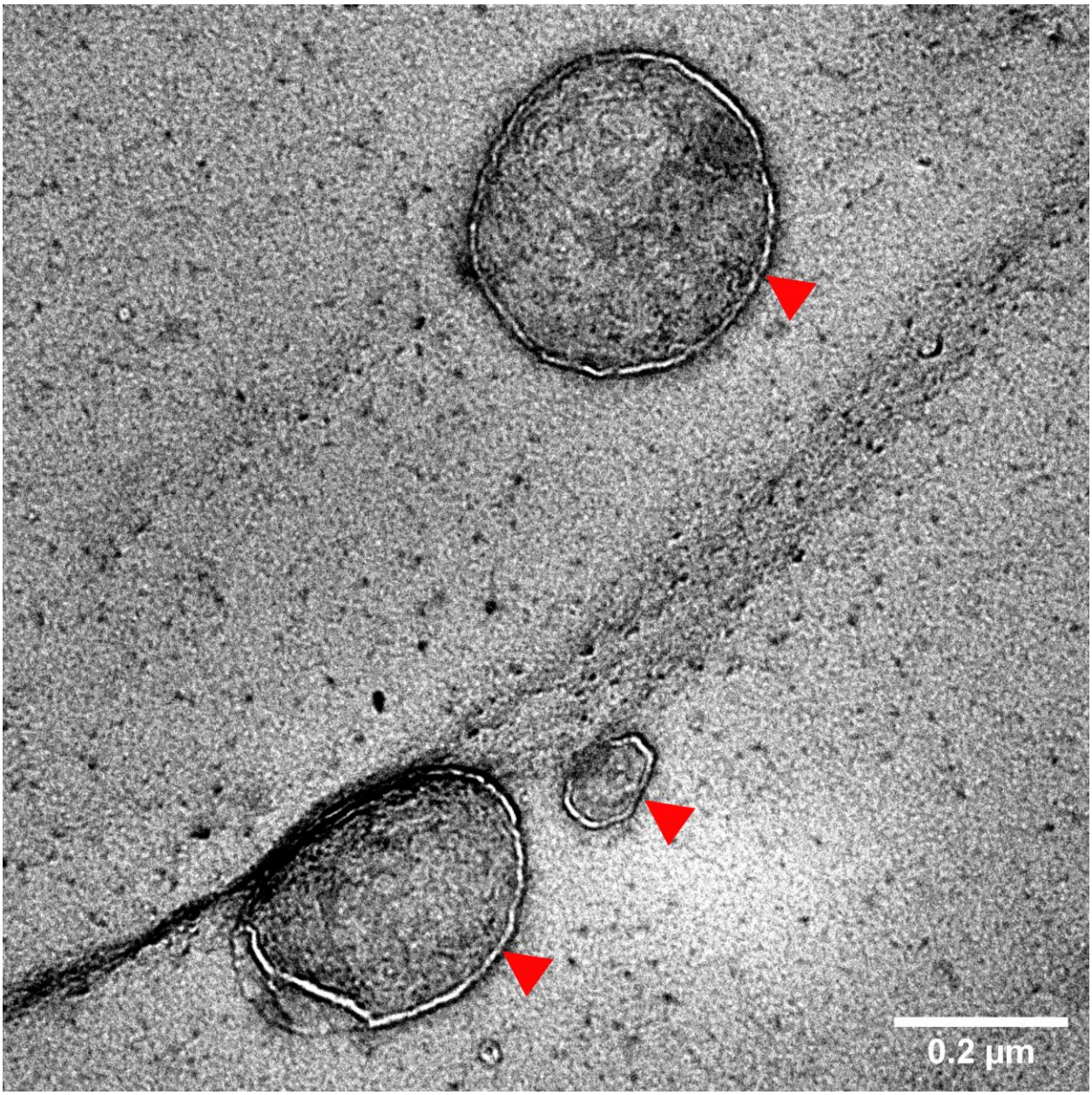

Supplementary figure 3. Transmission electron microscopy of decanoic acid:decanol (1:1) vesicles in PBS. Membranes are indicated by red arrows. Staining by uranium acetate. Thickiness of the membrane aligns with the expected range, and lumen is visible within a membrane. Scale bar - 200 nm.

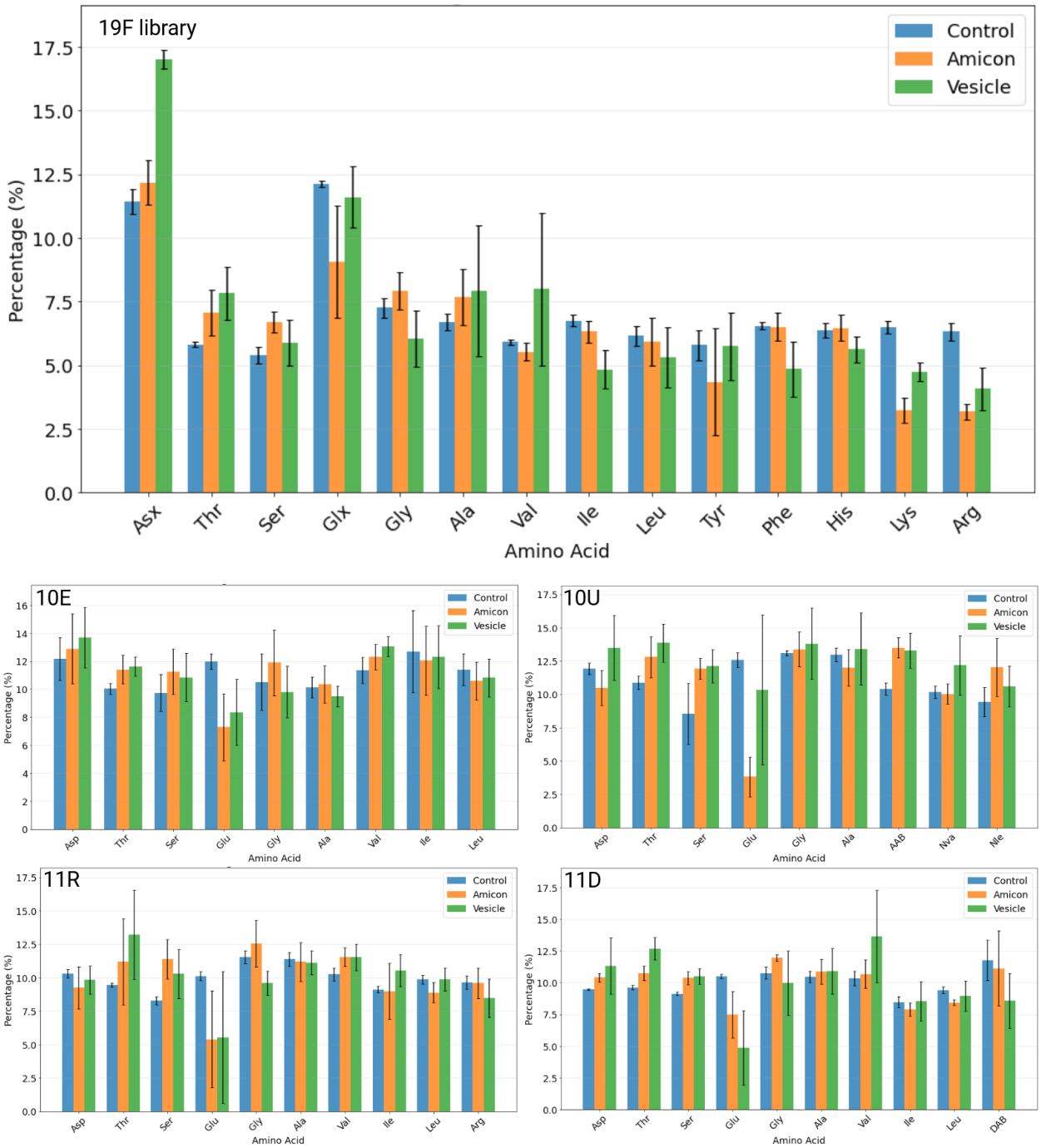

Supplementary figure 4. Amino acid distribution of random peptide libraries upon filtration through Amicon Ultra-4 3K centrifuge filters (orange bars) and upon incubation with DA:DOH vesicles with consequent filtration through Amicon Ultra-4 3K centrifuge filters (green bars). It appears that filtration through Amicon Ultra-4 3K filters mildly skews amino acid distribution of 8-mer peptide libraries, and, as such, it is difficult to derive conclusions on the changes of amino acid distribution of peptide library upon incubation with DA:DOH vesicles. Since Asp and Glu overlap with Asn and Gln on HPLC graph, they are pulled together at the amino acid distribution graphs for 19F and labelled Asx and Glx, respectively. Error bars represents standard deviation from hexaplicates.

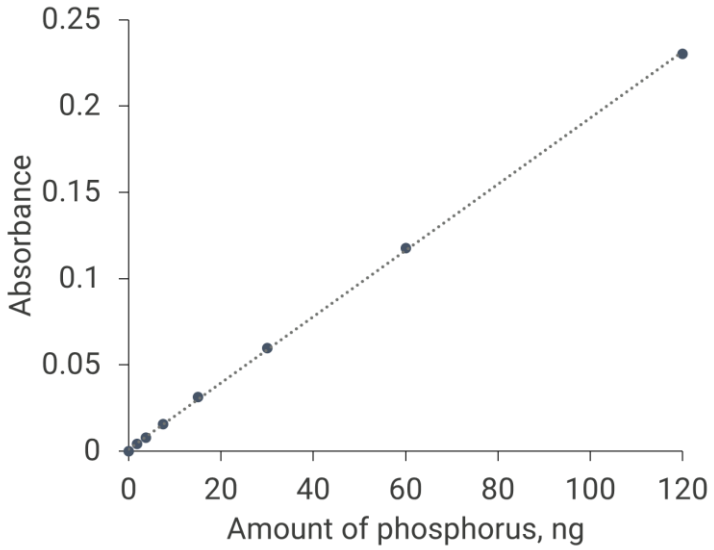

Supplementary Figure 5. Calibration curve used for measurement of phosphate release from fluorapatite using molybdenum blue spectrophotometric assay. The working concentration range from 3.75 to 150 ng of phosphorus (as $H_2PO_4^{2+}$).

	Control (no salts or peptides added)	DA:DOH vesicles + 363 mM NaCl	DA:DOH vesicles + 8.9 mM $MgCl_2$	DA:DOH vesicles + 1 mg/ml 10E library	DA:DOH vesicles + 1 mg/ml 11R library
ζ-potential (mV)	-54.586±2.647	-17.55±9.241	-32.6±2.453	-49.579±4.047	-46.166±2.75
Conductivity (mS/cm)	8.128±0.119	37.919±3.42	9.083±0.56	8.074±0.206	8.075±0.311
Quality Factor (signal/noise)	1.272±0.223	0.76±0.575	1.714±.083	1.227±0.131	1.867±0.837

Supplementary table 1. Table presenting ζ-potential and conductivity of DA:DOH vesicles under different conditions. ζ-potential of DA:DOH vesicles drops upon addition of salt and selected peptide libraries, indicating their potential role in vesicle flocculation (in case of NaCl), collapse (in case of $MgCl_2$) and binding/functional effects (in case of peptide libraries). Quality factor, as established by the Malvern Zetasizer instrument, represents signal to noise ratio of ζ-potential readings, with values above 0.9 considered to be of excellent quality and of 0.7-0.9 to be acceptable data with potential noise. We find higher noise in the sample with 363 mM NaCl, due to the increase in sample's conductivity and quick deterioration of the instruments' measuring cuvette by the electric current.